PHYSICAL REVIEW B **90**, 024423 (2014)

Orbital magnetic moment and coercivity of SiO_2-coated FePt nanoparticles studied by x-ray magnetic circular dichroism

Y. Takahashi,[1,*] T. Kadono,[1,†] S. Yamamoto,[2] V. R. Singh,[1,‡] V. K. Verma,[1,§] K. Ishigami,[3] G. Shibata,[1] T. Harano,[1]
Y. Takeda,[4] T. Okane,[4] Y. Saitoh,[4] H. Yamagami,[4,5] M. Takano,[2] and A. Fujimori[1,4]
[1]*Department of Physics, University of Tokyo, Bunkyo-ku, Tokyo 113-0033, Japan*
[2]*Institute for Integrated Cell-Material Science (iCeMS), Kyoto University, Yoshida Ushinomiya-cho, Sakyo-ku, Kyoto 606-8501, Japan*
[3]*Graduate School of Frontier Science, University of Tokyo, 7-3-1 Hongo, Bunkyo-ku, Tokyo 113-0033, Japan*
[4]*Japan Atomic Energy Agency Quantum Beam Science Directorate, 1-1-1 Kouto, Sayo-cho, Sayo-gun, Hyogo 679-5148, Japan*
[5]*Department of Physics, Kyoto Sangyo University, Motoyama, Kamigamo, Kita-ku, Kyoto-City 603-8555, Japan*

(Received 30 October 2013; revised manuscript received 1 June 2014; published 25 July 2014)

We have investigated the spin and orbital magnetic moments of Fe in FePt nanoparticles in the $L1_0$-ordered phase coated with SiO_2 by x-ray absorption spectroscopy (XAS) and x-ray magnetic circular dichroism (XMCD) measurements at the Fe $L_{2,3}$ absorption edges. Using XMCD sum rules, we evaluated the ratio of the orbital magnetic moment (M_{orb}) to the effective spin magnetic moment ($M_{\mathrm{spin}}^{\mathrm{eff}}$) of Fe to be $M_{\mathrm{orb}}/M_{\mathrm{spin}}^{\mathrm{eff}} = 0.08$. This $M_{\mathrm{orb}}/M_{\mathrm{spin}}^{\mathrm{eff}}$ value is comparable to the value (0.09) obtained for FePt nanoparticles prepared by gas phase condensation, and is larger than the values ($\sim$0.05) obtained for FePt thin films, indicating a high degree of $L1_0$ order. The hysteretic behavior of the FePt component of the magnetization was measured by XMCD. The magnetic coercivity (H_c) was found to be as large as 1.8 T at room temperature, $\sim$3 times larger than the thin film value and $\sim$50 times larger than that of the gas phase condensed nanoparticles. The hysteresis curve is well explained by the Stoner-Wohlfarth model for noninteracting single-domain nanoparticles with the H_c distributed from 1 to 5 T.

DOI: 10.1103/PhysRevB.90.024423 PACS number(s): 78.20.Ls, 75.60.−d, 75.50.Bb, 75.75.Fk

The $L1_0$-ordered alloy FePt has attracted great attention as a material to be used in high-density storage memory devices because FePt possesses a high magnetocrystalline anisotropy in bulk FePt and thin films [1–4]. In order to increase the storage density of memory devices, FePt nanoparticles are promising materials. FePt nanoparticles prepared by the gas phase preparation method [5] and the wet chemical preparation method [6], however, have the fcc structure, in which magnetocrystalline anisotropy disappears. By annealing the nanoparticles at high temperatures, one can transform its structure from the fcc to $L1_0$, but if the annealing time is not long enough to transform the entire FePt into the $L1_0$-ordered state, untransformed fcc FePt shows superparamagnetism and eventually reduces the magnetic anisotropy energy as is the case for FePt nanoparticles prepared by the gas-phase-condensed method followed by in-flight heat treatment [7], whose magnetic coercivity (H_c) is as small as 0.038 T [8]. In addition, high temperature annealing is difficult to implement in existing manufacturing process because it leads to the coalescence of nanoparticles into larger particles unless any precautions are made [9]. Recently, in order to overcome such difficulties, FePt nanoparticles coated with SiO_2 before annealing were prepared to achieve a high degree of $L1_0$ order [6,10–14]. FePt nanoparticles prepared by this method have a H_c as large as 1.85 T at 300 K [14], of the same order as the value of 3.0 T observed for $L1_0$-FePt (001) particulate films [15], and much larger than the bulk value of 0.16 T [16], the thin film value of 0.55 T [4], and the value of 0.75 T for microfabricated FePt (001) dots [17].

In order to understand the origin of the large H_c and to further improve the properties of the SiO_2-coated FePt nanoparticles, microscopic information about the magnetism such as the orbital magnetic moment is important. The chemical state of Fe can be easily distinguished by soft x-ray absorption spectroscopy (XAS), and the orbital and spin magnetic moments of transition-metal 3d orbitals can be measured by soft x-ray magnetic circular dichroism (XMCD) measurements of the 2p core level of the transition element [18]. Furthermore, in XMCD measurements, one can eliminate extrinsic magnetic signals such as those from oxidized Fe and those from the diamagnetic SiO_2 coating. In the present work we have applied the XAS and XMCD techniques to the SiO_2-coated FePt nanoparticles to characterize their magnetic properties from the microscopic level.

FePt nanoparticle samples were prepared by the wet chemical method. Precursor fcc FePt nanoparticles were prepared according to the method of Sun *et al.* [19], and were subsequently coated by SiO_2 according to the method of Fan *et al.* [20]. Thus, during the heat treatment thermal diffusion of Fe and Pt atoms was confined inside the SiO_2 nanoreactor. The particle composition was $Fe_{55}Pt_{45}$, and an average core size and its standard deviation were estimated to be 6.4 nm and 15%, respectively [14]. Transmission electron microscopy (TEM) pictures reported by Yamamoto *et al.* [14] indicate that the thickness of the SiO_2 coat is 10–15 nm. For details of the fabrication process, we refer the reader to Yamamoto *et al.* [14]. For the XMCD measurements, the

---

[*] Present address: Institute for Solid State Physics, University of Tokyo, Kashiwa, Chiba 277-8581, Japan; takahashi@issp.u-tokyo.ac.jp

[†] Present address: Department of Physical Sciences, Ritsumeikan University, Kusatsu, Shiga 525-8577, Japan.

[‡] Present address: Department of Physics and Astronomy, University of Nebraska-Lincoln, NE 68588-0299, USA.

[§] Present address: Department of Physics, Madanapalle Institute of Technology, and Science, Angallu, Madanapalle-517325, AP, India.

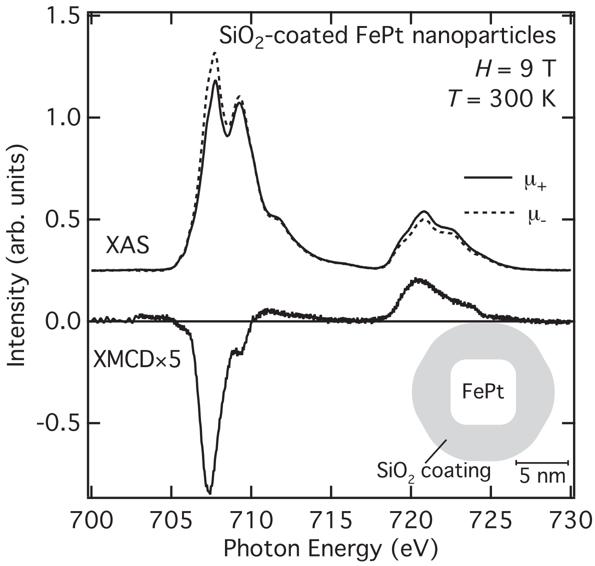

FIG. 1. XAS and XMCD spectra at the Fe $L_{2,3}$ edges of the SiO_2-coated FePt nanoparticles under the applied magnetic field of 9 T. All the spectra have been normalized to the L_3 XAS peak intensity. Inset shows a schematic figure of the FePt nanoparticle coated by SiO_2.

nanoparticle samples were supported by silver paste on a sample holder. After the preparation of the samples, they were kept in an Ar atmosphere in order to prevent oxidation until the XMCD measurements. XAS $[=(\mu_+ + \mu_-)/2]$ and XMCD $(=\mu_+ - \mu_-)$ spectra were obtained at the helical undulator beam line BL23SU of SPring-8. Here μ_+ and μ_- are XAS spectra taken with the light helicity parallel and antiparallel to the incident photon direction, respectively. The highest applied magnetic field was 9 T. The measurements were done under an ultrahigh vacuum of $\sim 4.8 \times 10^{-9}$ Pa. The polarity of the synchrotron radiation was switched at each photon energy using a kicker magnet with the frequency of 1 Hz [21]. The measurements were done at room temperature (∼300 K) in the total electron yield (TEY) mode. The magnetic field dependence of the XMCD intensity at the peak of the Fe L_3 edge was measured in the range of $-9 \leqslant H \leqslant 9$ T.

Figure 1 shows the XAS and XMCD spectra at the Fe $L_{2,3}$ edges of the FePt nanoparticles. All the spectra have been normalized to the L_3 XAS peak intensity. Unlike the Fe $L_{2,3}$ spectra of FePt by Boyen *et al.* [7] and Dmitrieva *et al.* [8], each of the L_3 and L_2 edges exhibits a doublet structure: The L_3 doublet peaks are located at 707.7 and 709.3 eV, and the L_2 ones at 720.8 and 722.7 eV. Furthermore, broad shoulder/tail structures are observed on the high-energy side of the L_3 peak from 710 to 717 eV and on the high-energy side of the L_2 peak from 722 to 730 eV. We consider that the origin of the doublets is overlapping signals of FePt (at 707.7 and 720.8 eV) and Fe oxides (at 709.3 and 722.7 eV). The oxides are most likely extrinsic Fe^{3+} oxides formed at the surface of bare FePt particles whose SiO_2 coating was removed when grinding the sample into fine powders, as one can see from the TEM picture [shown in Fig. 2(b) of Yamamoto *et al.* [14]]. We tentatively attribute the shoulder/tail structures to the charge-transfer $2p^5d^6$-$2p^5d^7\underline{L}$ satellite of the Fe^{3+} oxide [22] but the exact origin of the structure remains to be clarified. On the other hand, the line shape of the experimental XMCD spectrum in Fig. 1 is almost identical to that of FePt by Dmitrieva *et al.* [8] except for a small negative peak around 709 eV, indicating that contributions of the Fe oxides to the XMCD spectrum are small.

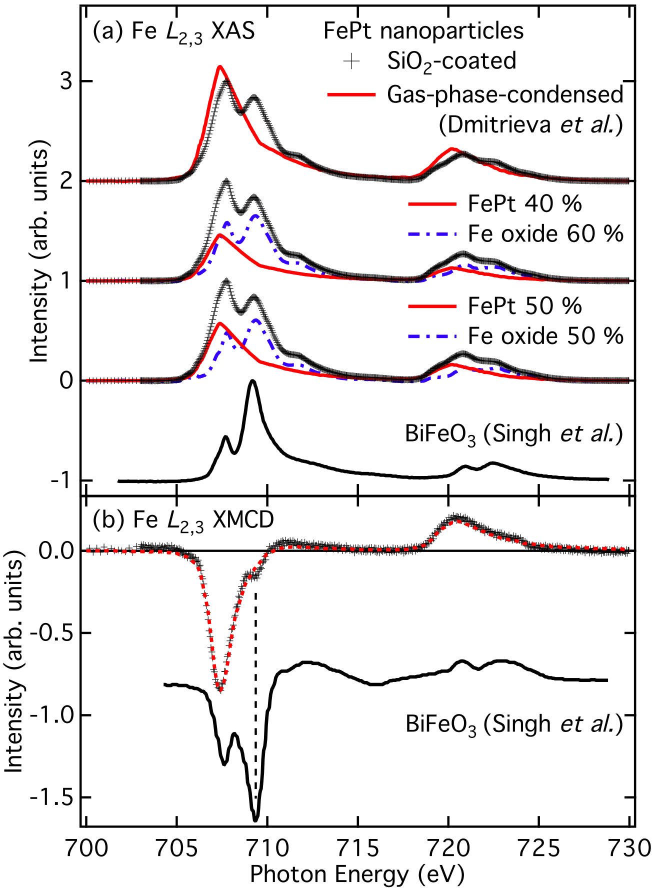

FIG. 2. (Color online) Decomposition of the measured XAS and XMCD spectra into those of FePt and a Fe^{3+} oxide. (a) The experimental XAS spectrum and that of gas-phase-condensed FePt nanoparticles [8] are shown by crosses and a solid curve, respectively, at the top. Spectra after subtraction of the FePt ones from the measured ones by different ratios are indicated below by dot-dashed curves. The XAS spectrum of $BiFeO_3$ by Singh *et al.* [23] is shown at the bottom. (b) The experimental XMCD spectrum (crosses) and the FePt one (Ref. [8], dotted curve) are shown at the top. The XMCD spectrum of $BiFeO_3$ by Singh *et al.* [23] is shown at the bottom.

In order to estimate signals of the Fe oxides, we first subtracted the FePt XAS spectrum reported by Dmitrieva *et al.* [8], where Fe oxide was completely removed by plasma treatment, from the experimental one. In Fig. 2(a) one can see that after having subtracted the FePt XAS spectrum multiplied by ∼0.5, the spectral line shape became similar to that of $BiFeO_3$, where the Fe^{3+} ion is located at the O_h site [23], shown in the bottom of Fig. 2(a). Thus the intrinsic signals from FePt are estimated to be 50% of the total Fe $L_{2,3}$ XAS intensity. The experimental XMCD spectrum at the Fe $L_{2,3}$ edges of the FePt nanoparticles is shown in Fig. 2(b). The line shape of the XMCD spectrum of FePt nanoparticles prepared by the gas condensation method by Dmitrieva *et al.* [8] is also

TABLE I. Values of the effective spin ($M_{\rm spin}^{\rm eff}$) and orbital ($M_{\rm orb}$) magnetic moments (in units of μ_B/Fe) and the coercive field H_c (in units of T) for different FePt samples.

	$M_{\rm spin}^{\rm eff}$	$M_{\rm orb}$	$M_{\rm orb}/M_{\rm spin}^{\rm eff}$	H_c
Nanoparticle (present work)	1.4	0.12	0.08	1.8
Nanoparticle (gas phase) [8]	2.21	0.19	0.09	0.038
FePt thin films [26]	0.5	0.025	0.05 ± 0.01	0.1

shown by a dotted curve. Unlike the XAS spectra, both XMCD data agree with each other except for the small negative peak around 709 eV in the present sample. From comparison of the present XMCD spectrum with the XMCD spectrum of $BiFeO_3$ shown at the bottom of Fig. 2(b), the small negative peak can be attributed to a peak of a Fe^{3+} oxide. After having removed the Fe-oxide contributions from the experimental XAS and XMCD spectra, we applied the XMCD sum rules [18,24] and estimated the effective spin magnetic moment $M_{\rm spin}^{\rm eff}$, which is the sum of the spin magnetic moment and the magnetic dipole moment, to be 1.4 μ_B/Fe, the orbital magnetic moment $M_{\rm orb} = 0.12$ μ_B/Fe, and their ratio $M_{\rm orb}/M_{\rm spin}^{\rm eff} = 0.08$ [25]. These values are summarized in Table I, and are compared with those of different kinds of FePt samples [8,26]. The obtained $M_{\rm orb}/M_{\rm spin}^{\rm eff}$ ratio is comparable to the value (0.09) obtained for FePt nanoparticles prepared by gas phase condensation [8], and is larger than the values ($\sim$0.05) obtained for FePt thin films [26], indicating a high degree of $L1_0$ order. The deduced $M_{\rm spin}^{\rm eff} = 1.4$ μ_B/Fe is, however, small compared to the other FePt samples ($\geqslant$2 μ_B/Fe). The origin of this discrepancy is not clear at present, but the outermost layers of the bare FePt particles might also be oxidized to Fe^{2+} and become nonferromagnetic because the XAS and XMCD line shapes of Fe^{2+} oxides and metallic Fe are hardly distinguishable.

Figure 3(a) shows the Fe L_3-edge XMCD intensities of the FePt nanoparticles as functions of magnetic field at two different photon energies. The curve at $h\nu = 709.2$ eV, which reflects the XMCD signal of the Fe^{3+} oxide, is linear in H and shows no hysteretic behavior. Since the slope is given by the magnetic susceptibility χ of the Fe^{3+} ion of the oxide, it is given by C/T if the Fe^{3+} ion is paramagnetic or by C/T_N if it is antiferromagnetic. Here C and T_N are the Curie constant for the Fe^{3+} ($S = 5/2$) ion and the Neel temperature, respectively. From the slope $\chi \sim 0.023$ μ_B/T, we estimated T or $T_N \sim C/\chi = 325$ K, indicating that the Fe^{3+} at 300 K are paramagnetic or slightly below T_N, and cannot be ferro/ferrimagnetic.

In contrast, the XMCD intensity at $h\nu = 707.7$ eV, which is dominated by FePt, shows a hysteretic behavior with H_c of 1.8 T. Because a M-H curve of the peak of the Fe oxides overlaps with the curve at $h\nu = 707.7$ eV, we obtained a M-H curve of a ferromagnetic component by subtracting the curve at $h\nu = 709.2$ eV from the curve at $h\nu = 707.7$ eV. From the shape of the hysteresis loop thus obtained, as shown in Fig. 3(a), one can see that the value of the remnant magnetization is half of that of the saturation magnetization and the shape itself is somewhat rounded compared to a typical rectangular hysteresis loop for ferromagnetic materials. These behaviors are characteristic of the hysteresis of the Stoner-Wohlfarth model [27,28], which explains H_c based on the coherent reversal in noninteracting single-domain particles and in good agreement with some reports of nanoparticle magnetism [29,30]. Therefore, we first introduced the Stoner-Wohlfarth model with a fixed H_c (=2.5 T) to reproduce the measured hysteresis loop, however, we could not obtain a good fit as shown by a dashed curve in Fig. 3(b), because the experimental curve was broader in the high-field region. Then we assumed a distribution of H_c over a finite range (we assumed the log-normal distribution) as shown in the inset of Fig. 3(b). The calculated hysteresis loop shown in Fig. 3(b) reproduces almost all the characteristics of the experimental curve, indicating that the SiO_2-coated FePt nanoparticles act as noninteracting single-domain particles whose H_c is distributed from $\sim$1 to $\sim$5 T.

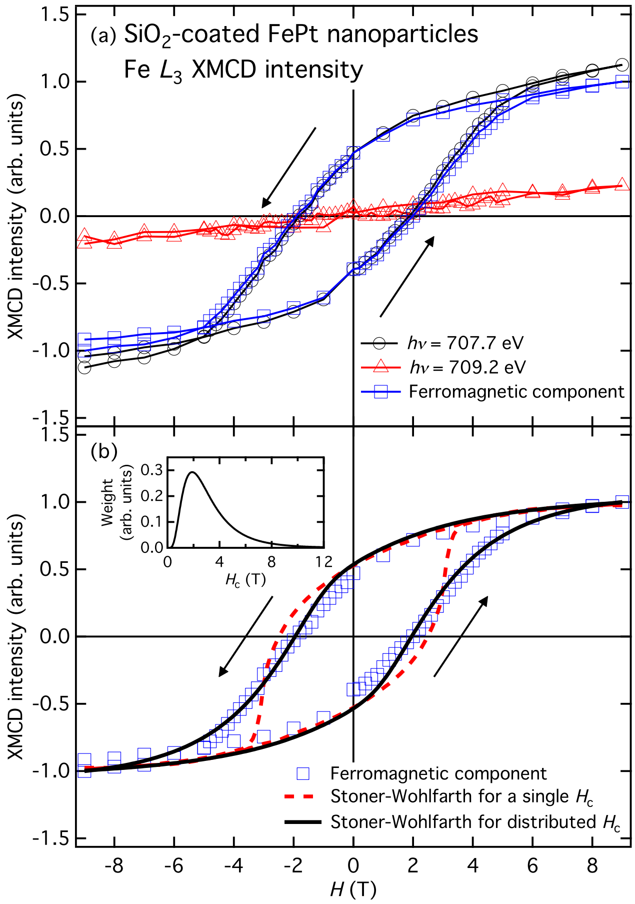

FIG. 3. (Color online) Hysteresis loops of the XMCD intensities (normalized to the saturation magnetization) at the Fe L_3 edge of the SiO_2-coated FePt nanoparticles. (a) Hysteresis loops at $h\nu = 707.7$ eV (open circles) and 709.2 eV (open triangles) corresponding to a peak due to FePt and the Fe^{3+} oxides, respectively. A ferromagnetic component extracted from the hysteresis loop at $h\nu = 707.7$ eV (open squares) is also plotted. (b) The ferromagnetic component of the XMCD hysteresis curve compared with a calculated Stoner-Wohlfarth hysteresis loop [27] for a single H_c (=2.5 T) (dashed curve) and for distributed H_c (solid curve). Inset shows the log-normal distribution of H_c normalized to the area.

Now let us discuss the magnitude of the uniaxial magnetic anisotropy energy and the origin of the distribution of H_c. In the Stoner-Wohlfarth model for an assembly of noninteracting particles whose anisotropy axes are randomly oriented, the H_c is given by the following equation [27]:

$$\begin{aligned} H_c &= 0.482 \frac{2K_\mathrm{u}}{\mu_0 M_\mathrm{s}} \\ &= 0.482 \left(\frac{2K_1}{\mu_0 M_\mathrm{s}} + \frac{1-3\mathcal{N}}{2} M_\mathrm{s} \right), \end{aligned} \tag{1}$$

where K_u, μ_0, M_s, K_1, and $\mathcal{N}$ are the uniaxial magnetic anisotropy energy per unit volume, the vacuum permeability, the saturation magnetization, the magnetocrystalline anisotropy energy per unit volume, and the demagnetizing factor, respectively. In Eq. (1), the first and second terms originate from the magnetocrystalline anisotropy and the shape anisotropy of each particle, respectively. Using the mean value $H_c = 3.25$ T and $M_\mathrm{s} = 2.4\ \mu_\mathrm{B}/\mathrm{Fe}$ for the oxide-free FePt nanoparticles [8], the value of K_u is estimated to be $2.7 \times 10^6\ \mathrm{J/m^3}$. This value is of the same order of magnitude as that of thin films $3.0 \times 10^6\ \mathrm{J/m^3}$ [31] and several times larger than that of the gas-phase-condensed FePt nanoparticles $6.0 \times 10^5\ \mathrm{J/m^3}$ [8]. As for the origin of the distribution of H_c, because the $\mathcal{N}$ value changes between 0 and 1 depending on the shape of each particle, the value of the second term in Eq. (1) varies from -0.49 to 0.24 T assuming $M_\mathrm{s} = 2.4\ \mu_\mathrm{B}/\mathrm{Fe}$ [8]. Furthermore, too small particles may suffer from superparamagnetic fluctuations of the magnetization due to their small magnetic anisotropy energy per particle. These might originate from the distribution of the particle sizes and could possibly explain the distribution of H_c obtained for the present sample.

Finally, we discuss the possibility of the observed large H_c value for the SiO$_2$-coated FePt nanoparticles. The maximum single-domain size R_sd is estimated as $R_\mathrm{sd} \approx 9\sqrt{\frac{k_\mathrm{B}T_\mathrm{C}}{2a_0} K_1}/\mu_0 M_\mathrm{s}^2$, where k_B, T_C, and a_0 are Boltzmann constant, Curie temperature, and the lattice constant, respectively [27]. Using typical values for FePt nanoparticles of $K_1 \sim 10^6\ \mathrm{J/m^3}$ [32], $a_0 = 0.386$ nm [33], and $M_\mathrm{s} = 2.4\ \mu_\mathrm{B}/\mathrm{Fe}$ [8], we estimate the lower limit of R_sd as $\sim$100 nm, orders of magnitude larger than the particle size. Therefore, the SiO$_2$-coated FePt nanoparticles can form in single domains and in our fabrication method, the SiO$_2$ coating protects the small enough FePt nanoparticle from extra dispersion, deterioration, and oxidization during the sample preparation, leading to isolated single-domain FePt particles, and eventually to the large H_c value.

In conclusion, we have investigated the spin and orbital magnetic moments of Fe in FePt nanoparticles coated with SiO$_2$ using XMCD measurements. The deduced ratio of the orbital to effective spin magnetic moments $M_\mathrm{orb}/M_\mathrm{spin}^\mathrm{eff} = 0.08$ is nearly equal to that of FePt nanoparticles (0.09) condensed from gas phase for which oxidized layers were removed by *in situ* plasmas treatment [8]. The magnetization measured by Fe L_3-edge XMCD was saturated around 6 T and H_c was as large as 1.8 T, much larger than the H_c ($\sim$0.038 T) of the gas phase condensed samples [8], and consistent with the result of the SQUID measurement [14]. The XMCD intensity versus magnetic field curve was fitted to the Stoner-Wohlfarth model for noninteracting single-domain nanoparticles whose H_c is distributed between $\sim$1 and $\sim$5 T.

This work was supported by a Grant-in-Aid for Scientific Research from the JSPS (S22224005) and the "Quantum Beam Technology Development Program" of JST. The experiment was done under the approval of the Photon Factory Program Advisory Committee (Proposal No. 2010G187), under the Shared Use Program of JAEA Facilities (Proposal No. 2011A3840), and at JAEA beamline in SPring-8 (Proposals No. 2011B3823 and No. 2012A3823/BL23-SU). S.Y. acknowledges financial support from MEXT KAKENHI (20104006). Y.T. was supported by JSPS through the Program for Leading Graduate Schools (MERIT).

---

[1] O. A. Ivanov, L. V. Solina, V. A. Demshina, and L. M. Magat, Phys. Met. Metallogr. **35**, 81 (1973).

[2] S. Okamoto, N. Kikuchi, O. Kitakami, T. Miyazaki, Y. Shimada, and K. Fukamichi, Phys. Rev. B **66**, 024413 (2002).

[3] T. Seki, S. Mitani, K. Yakushiji, and K. Takanashi, Appl. Phys. Lett. **88**, 172504 (2006).

[4] T. Seki, S. Mitani, and K. Takanashi, Phys. Rev. B **77**, 214414 (2008).

[5] O. Dmitrieva, M. Acet, G. Dumpich, J. Kästner, C. Antoniak, M. Farle, and K. Fauth, J. Phys. D: Appl. Phys. **39**, 4741 (2006).

[6] S. Yamamoto, Y. Morimoto, Y. Tamada, Y. K. Takahashi, K. Hono, T. Ono, and M. Takano, Chem. Mater. **18**, 5385 (2006).

[7] H.-G. Boyen, K. Fauth, B. Stahl, P. Ziemann, G. Kästle, F. Weigl, F. Banhart, M. Hessler, G. Schütz, N. Gajbhiye, J. Ellrich, H. Hahn, M. Büttner, M. Garnier, and P. Oelhafen, Adv. Mater. **17**, 574 (2005).

[8] O. Dmitrieva, M. Spasova, C. Antoniak, M. Acet, G. Dumpich, J. Kästner, M. Farle, K. Fauth, U. Wiedwald, H.-G. Boyen, and P. Ziemann, Phys. Rev. B **76**, 064414 (2007).

[9] S. Sun, S. Anders, T. Thomson, J. E. E. Baglin, M. F. Toney, H. F. Hamann, C. B. Murray, and B. D. Terris, J. Phys. Chem. B **107**, 5419 (2003).

[10] Y. Morimoto, Y. Tamada, S. Yamamoto, M. Takano, and T. Ono, J. Magn. Soc. Jpn. **30**, 464 (2006).

[11] Y. Tamada, Y. Morimoto, S. Yamamoto, N. Hayashi, M. Takano, S. Nasu, and T. Ono, Jpn. J. Appl. Phys. **45**, L1232 (2006).

[12] Y. Tamada, S. Yamamoto, M. Takano, S. Nasu, and T. Ono, Appl. Phys. Lett. **90**, 162509 (2007).

[13] Y. Tamada, Y. Morimoto, S. Yamamoto, M. Takano, S. Nasu, and T. Ono, J. Magn. Magn. Mater. **310**, 2381 (2007).

[14] S. Yamamoto, Y. Morimoto, T. Ono, and M. Takano, Appl. Phys. Lett. **87**, 032503 (2005).

[15] D. Wang, T. Seki, K. Takanashi, T. Shima, G. Li, H. Saito, and S. Ishio, J. Appl. Phys. **105**, 07A702 (2009).

[16] Y. Tanaka, N. Kimura, K. Hono, K. Yasuda, and T. Sakurai, J. Magn. Magn. Mater. **170**, 289 (1997).

[17] D. Wang, T. Seki, K. Takanashi, and T. Shima, J. Phys. D: Appl. Phys. **41**, 195008 (2008).

[18] B. T. Thole, P. Carra, F. Sette, and G. van der Laan, Phys. Rev. Lett. **68**, 1943 (1992).

[19] S. Sun, C. B. Murray, D. Weller, L. Folks, and A. Moser, Science **287**, 1989 (2000).

[20] H. Fan, K. Yang, D. M. Boye, T. Sigmon, K. J. Malloy, H. Xu, G. P. López, and C. J. Brinker, Science **304**, 567 (2004).

[21] Y. Saitoh, Y. Fukuda, Y. Takeda, H. Yamagami, S. Takahashi, Y. Asano, T. Hara, K. Shirasawa, M. Takeuchi, T. Tanaka, and H. Kitamura, J. Sync. Rad. **19**, 388 (2012).

[22] J. P. Crocombette, M. Pollak, F. Jollet, N. Thromat, and M. Gautier-Soyer, Phys. Rev. B **52**, 3143 (1995).

[23] V. R. Singh, V. K. Verma, K. Ishigami, G. Shibata, Y. Yamazaki, A. Fujimori, Y. Takeda, T. Okane, Y. Saitoh, H. Yamagami, Y. Nakamura, M. Azuma, and Y. Shimakawa, J. Appl. Phys. **114**, 103905 (2013).

[24] P. Carra, B. T. Thole, M. Altarelli, and X. Wang, Phys. Rev. Lett. **70**, 694 (1993).

[25] This ratio might become larger if corrections were made for the TEY saturation effects, however, the existence of the SiO_2 coat almost hindered the quantitative correction.

[26] S. Imada, A. Yamasaki, S. Suga, T. Shima, and K. Takanashi, Appl. Phys. Lett. **90**, 132507 (2007).

[27] J. M. D. Coey, *Magnetism and Magnetic Materials* (Cambridge University Press, Cambridge, 2010).

[28] E. C. Stoner and E. P. Wohlfarth, Philos. Trans. R. Soc. London Ser. A **240**, 599 (1948).

[29] M. Chuev, J. Exp. Theor. Phys. Lett. **85**, 611 (2007).

[30] L.-M. Lacroix, R. B. Malaki, J. Carrey, S. Lachaize, M. Respaud, G. F. Goya, and B. Chaudret, J. Appl. Phys. **105**, 023911 (2009).

[31] T. Seki, H. Iwama, T. Shima, and K. Takanashi, J. Phys. D: Appl. Phys. **44**, 335001 (2011).

[32] N. A. Usov and J. M. Barandiaran, Appl. Phys. Lett. **101**, 172402 (2012).

[33] T. J. Klemmer, N. Shukla, C. Liu, X. W. Wu, E. B. Svedberg, O. Mryasov, R. W. Chantrell, D. Weller, M. Tanase, and D. E. Laughlin, Appl. Phys. Lett. **81**, 2220 (2002).